# Activated dendritic cells delivered in tissue compatible biomatrices induce *in-situ* anti-tumor CTL responses leading to tumor regression

## Supplementary Materials

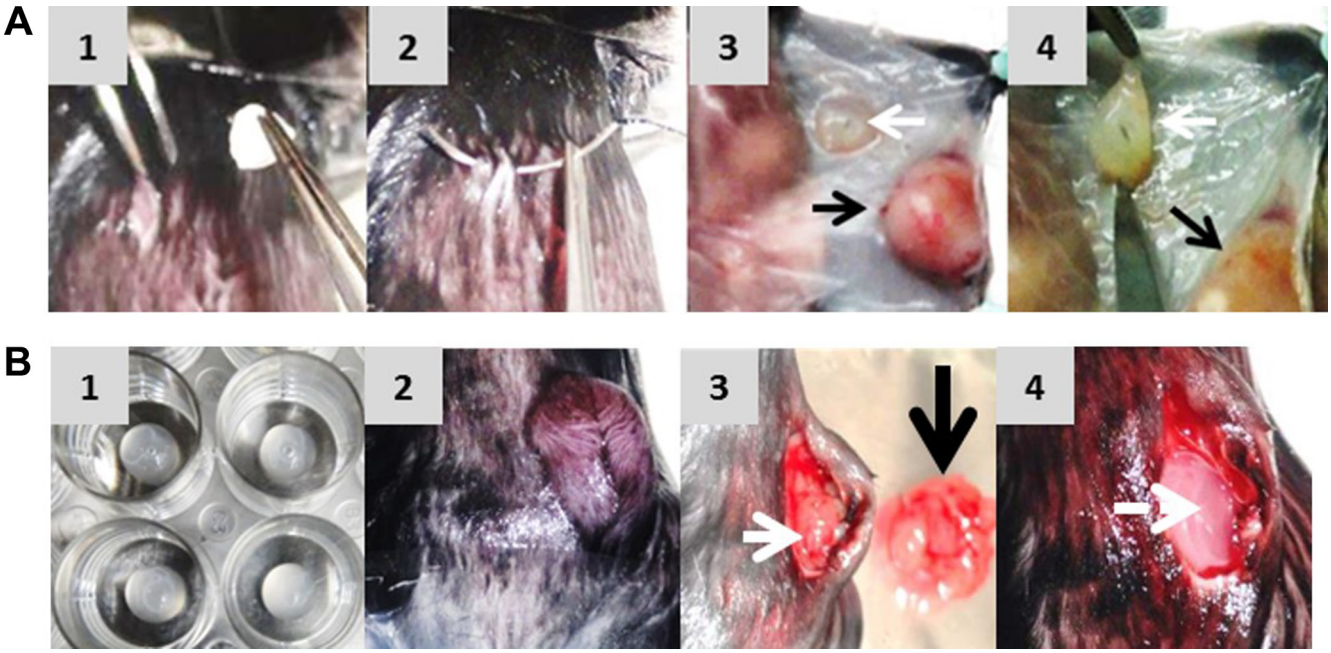


**Supplementary Figure S1: Generation of DC scaffolds for tumor treatment.** (**A**) Panel 1 shows the placement of DC scaffolds near the tumor site, panel 2 depicts the closing of the wound while panel 3 shows the physiological appearance of biomatrix 2–3 weeks post-implantation, and panel 4 shows the procedure of biomatrix harvesting along with host reactive tissue. White arrows show the biomatrix while black arrow shows the tumor mass. (**B**) Panel 1 shows the formation of flat DC scaffolds for the treatment of post-surgery secondary tumors. Panel 2 shows the tumor mass at the time of resection. Panel 3 shows the cavity created by the tumor resection (white arrow) and the removed tumor mass (black arrow). Panel 4 shows the placement of DC scaffold into the cavity for tumor treatment.

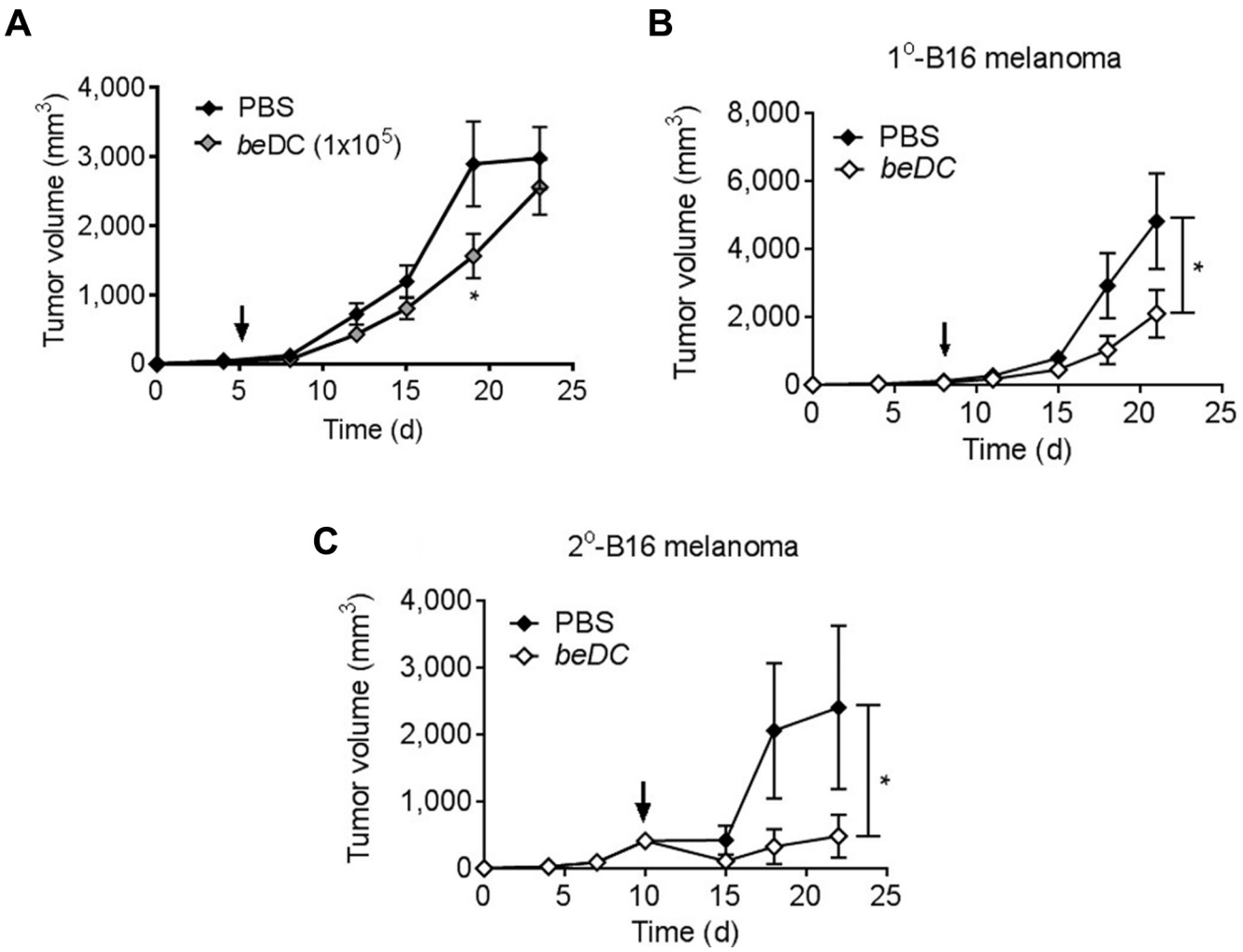


**Supplementary Figure S2: (A)** Treatment of TC1 tumors with biomatrix carrying $1 \times 10^5$ DCs. Treatment of B16 cell induced 1° (**B**) or 2° (**C**) melanoma using DC scaffolds. $n = 5–10$. Black arrow in A indicates the time point of commencement of therapy while black arrow in B represents the time point of tumor resection and DC-scaffold implantation. Data is represented as + SEM. *$p$-value < 0.05.

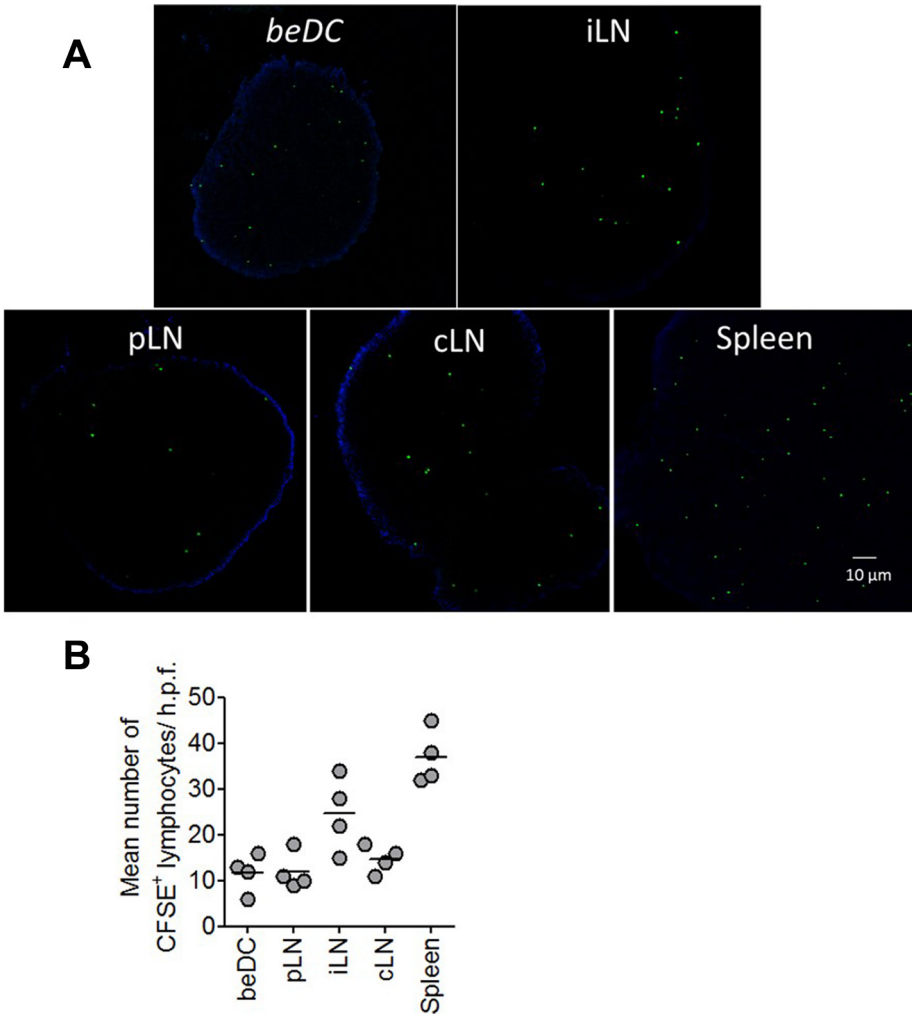


**Supplementary Figure S3: Adoptively transferred lymphocytes reach host-implanted DC scaffolds with equal propensity compared with other SLOs.** (**A**) Representative figures showing the relative movement of $CFSE^+$ lymphocytes into the biomatrix or SLOs 48 hours after adoptive transfer. iLN, inguinal lymph node; pLN, popliteal lymph node; cLN, cervical lymph node. (**B**) Quantification of infiltrating lymphocytes in high power fields.

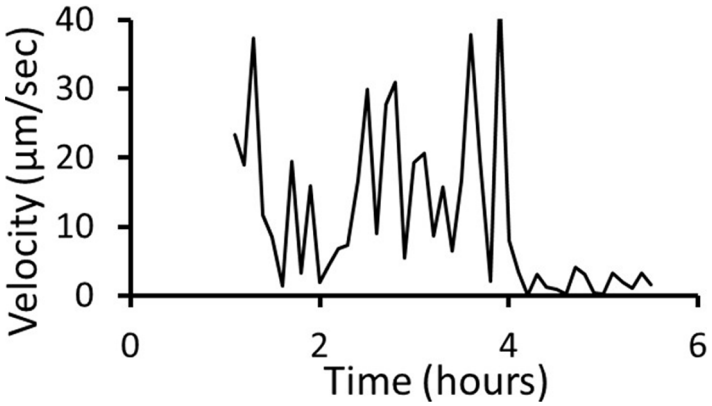


**Supplementary Figure S4: Velocity of migrating lymphocytes inside the biomatrices under *in vitro* conditions.** $CFSE^+$ lymphocytes and Q $dot^+$ DCs were put together in the scaffold and imaged using a live imaging system. The velocity was calculated using the MatLab® software.

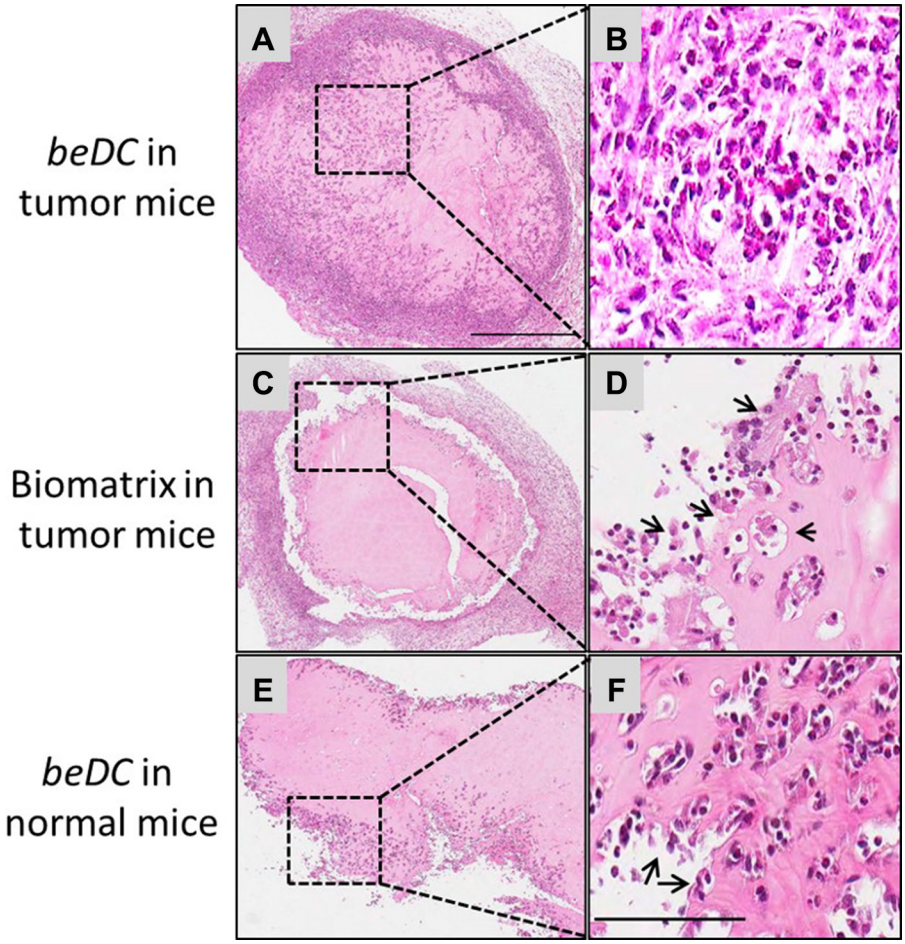


**Supplementary Figure S5: Hematoxylin and eosin staining of biomatrices harvested from various treatment groups.** (**A**, **C**, and **E**) are the 4x view of implants as depicted in the picture while (**B**, **D**) and (E) are the respective highlighted 40× areas. Black arrows in (**D** and **F**) show the sites of fibrin digestion by polymorphonuclear cells. Bar in A is equivalent to 1 mm while bar in (F) is equivalent to 100 μm.

**Supplementary Movie S1: Interaction of DCs in biomatrix with infiltrating host lymphocytes.** Though the DCs in scaffolds were stationary, the dendrites projected from them were making active physical contacts with infiltrating lymphocytes. See Supplementary_ Movie_S1

**Supplementary Movie S2: Movement of infiltrated lymphocytes inside the biomatrix.** Infiltrated host lymphocytes moved agilely and made intimate contacts with DCs for extended periods. See Supplementary_ Movie_S2

**Supplementary Movie S3: Cell division of infiltrated lymphocytes in association with DCS inside the biomatrix.** See Supplementary_ Movie_S3